SIMULATIONS OF ELECTRON CLOUD BUILD-UP AND SATURATION IN THE APS*

K. C. Harkay and R. A. Rosenberg, ANL, Argonne, IL 60439, USA†
M. A. Furman and M. Pivi, LBNL, Berkeley, CA 94720, USA‡

Abstract

In studies with positron beams in the Advanced Photon Source, a dramatic amplification was observed in the electron cloud for certain bunch current and bunch spacings. In modeling presented previously, we found qualitative agreement with the observed beam-induced multipacting condition, provided reasonable values were chosen for the secondary electron yield parameters, including the energy distribution. In this paper, we model and discuss the build-up and saturation process observed over long bunch trains at the resonance condition. Understanding this saturation mechanism in more detail may have implications for predicting electron cloud amplification, multipacting, and instabilities in future rings.

1 INTRODUCTION

In recent years, numerous observations of electron cloud effects (ECEs) have been reported in high-energy particle accelerators or storage rings, in some cases after operating them in new configurations [1]. These effects range in severity from vacuum degradation to emittance blowup, and generally become noticed when they degrade the accelerator performance. One of the many challenges in predicting beam-cloud interactions is understanding the electron cloud generation. A code developed at LBNL, POSINST, models the various processes giving rise to the cloud [2]. Uncertainties in characterizing the surface properties of the vacuum chamber, especially relating to secondary electron emission, can lead to uncertainties in the predicted cloud density. The goal of this modeling effort is to benchmark the code POSINST against measurements of the electron cloud (EC) properties undertaken at the Advanced Photon Source (APS), thereby providing realistic limits on the critical input parameters.

Dedicated electron diagnostics known as retarding-field analyzers (RFAs), first designed and implemented at the APS [3,4], were used in a series of experiments designed to study electron cloud effects induced by both positron and electron beams. As previously reported, a dramatic amplification was observed in the EC for certain bunch current and bunch spacings for positron beams [5]. This gain is attributed to beam-induced multipacting (BIM) and was accompanied by an anomalous vacuum pressure rise. A more modest amplification was observed for electron beams. In addition, before converting the APS to electron beam operation, a horizontal coupled-bunch instability was observed for positron beams at BIM conditions. This has not been observed for electron beams at identical operating conditions. In fact, ECEs do not limit the APS performance when operated with electrons, as is presently the case.

In previous modeling of positron beams [6], we found qualitative agreement with the observations for the BIM condition. Reasonable values were chosen for the secondary electron (SE) yield coefficient, the SE energy distribution, and the rediffused electron component. These assumptions are consistent with bench measurements [7,8]. Using these same input parameters, we then modeled the EC build-up and saturation process observed over long bunch trains at the resonance condition. It is hoped that this effort will lend insights into EC production in the APS, that can then be applied to other machines.

Three preliminary observations can be made: (1) the electron cloud is sensitive to details of the secondary electron energy spectrum, (2) the correct choice of these parameters should reproduce all the experimental data in a given machine, and (3) the measured longitudinal variation of the electron cloud density, which could be important, is not modeled.

2 REVIEW OF PRIOR RESULTS

A special vacuum chamber, equipped with ten RFA electron energy analyzers, was built and installed in a field-free region in the APS storage ring [5]. The locations of some of the components are shown in Fig. 1. EA6 is a copper end absorber designed to intercept high-energy photons to protect downstream structures. The schematic in Fig. 2 shows two RFAs mounted on a standard-aperture chamber. The approximate limits of the radiation fan at the location of detector 6 are shown for synchrotron photon energies above the photoelectron work function,

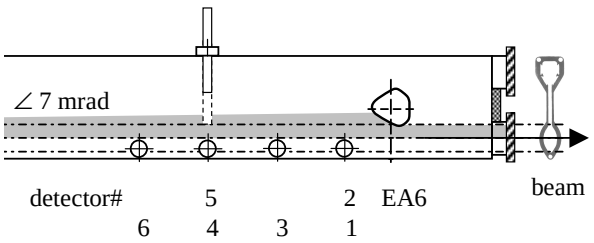

Figure 1: RFA detectors (1-6) mounted on APS chamber, top view, also showing the synchrotron radiation fan from the downstream bending magnet and the absorber, EA6.

*Work supported by U.S. Department of Energy, Office of Basic Energy Sciences under Contract Nos. W-31-109-ENG-38 and DE-AC03-76SF00098, and by the SNS project.
† harkay@aps.anl.gov and rar@aps.anl.gov
‡ mafurman@lbl.gov and mpivi@lbl.gov

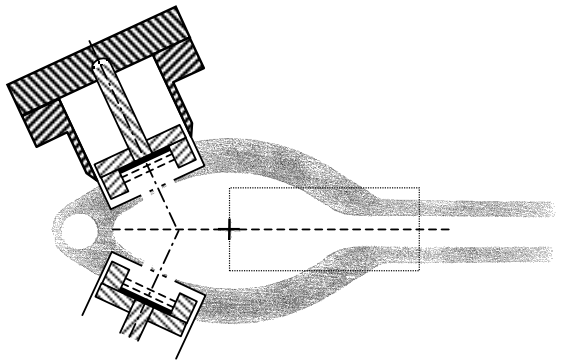

Figure 2: Mounting of two RFAs on a standard aluminum (Al) APS chamber, cross-sectional view. The RFA consists of two grids and a graphite-coated collector biased at +45V. The first grid is grounded and the second can be biased for electron energy selection [3,4].

~ 4 eV. Most of the high-energy photons exit through the antechamber slot.

The relevant APS parameters used in the previous [6] and present simulations are shown in Table 1. The parameter δ_{max} gives the maximum value of the secondary electron yield coefficient, which occurs at an incident energy E_{max}. Because the APS data were acquired over a long period of operation, we are interested in modeling the effects of surface conditioning by beam scrubbing, which lowers δ_{max}. Values of δ_{max} ranging from 2.2 to 3.3 are consistent with conditioned and unconditioned, oxidized Al, respectively.

Table 1: Simulation Parameters for APS

		BIM, Ref. [6]	EC build-up
Circumference	m	1104	
Beam energy	GeV	7	
Harmonic no.		1296	
Rf frequency	MHz	351.93	
Bunch population	(2 mA)	4.6×10^{10}	
rms bunch length	mm	5	
Transverse rms sizes	μm	300, 50	
Chamber semiaxes	cm	4.25, 2.1	
Antechamber slot height	cm	1	
Eff. photoelect. yield		0.1	
No. photons per e+		0.07	
δ_{max}		3.3	3.0 & 2.2
E_{max}	eV	280	300
No. kicks over bunch		5	11

The simulations in Ref. [6] were repeated with a slight modification (δ_{max} = 3.1). Also, the code output was scaled to account for the transmission attenuation in the experiment: The measured RFA grid transmission is 0.8, while the calculated transmission through the vacuum penetration is 0.6, giving a total detection efficiency of 0.5. Figure 3 shows a comparison between the modeled and measured electron wall current for ten positron bunches as a function of bunch spacing. The retarding voltage is positive to maximize the collector current. The model reproduces the broad peak centered around a 20-ns spacing (7 λ_{rf}); however, the sharp, resonant peak at 7 λ_{rf} is not reproduced. The position of the peak in the modeled result was very sensitive to the shape of the secondary electron energy spectrum, the mean energy in particular. The width of the broad peak was sensitive to assumptions about the rediffused electron component. It is interesting to note that BIM was never observed until the dedicated EC study: standard user operation with positron beams typically used 1 λ_{rf} or 54 λ_{rf} bunch spacing, well outside the position of the resonant peak.

The data in the main plot in Fig. 3 were acquired shortly after the new chamber was installed (< 1 Amp-hours (Ah) of operation). The inset shows the normalized signal after > 60 Ah. The peak signal is reduced by a factor of two due to a surface conditioning effect. The accumulated electron dose (in C/mm^2) was calculated using the measured wall current for the standard user configuration, assuming this was used the majority of the time. In the next section, we describe studies of the EC build-up over long bunch trains. The bunch train data were acquired after ~100 Ah, so we expect that δ_{max} may be further reduced relative to the initial state.

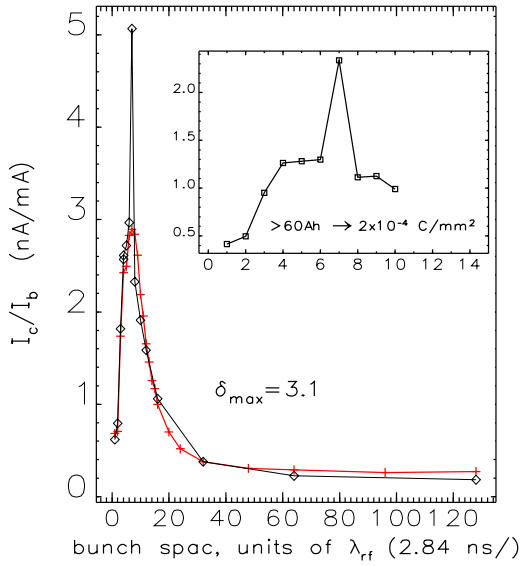

Figure 3: Measured (diamonds) and simulated (crosses) electron wall current (I_c) for BIM in APS, normalized to the total beam current (I_b) (ten e+ bunches; 2 mA/bunch).

3 MEASURED ELECTRON CLOUD BUILD-UP

Before discussing the electron cloud build-up and saturation, it should be noted that significant variation was seen from one detector to another, especially for BIM conditions [5]. The gain in the detector signals as a function of bunch spacing or number of bunches varied according to location. Detectors near the absorber EA6 typically exhibited the smallest gains (factors of 2-3),

while detectors 6, 7, and 8 exhibited gains of over a factor of 100. The effect of EA6 as a local source of electrons dominates in the detectors nearby. Farther from EA6, the situation is dramatically different, and the effect of multipacting is more easily observed.

Measurements of the electron cloud build-up and saturation are shown in Fig. 4. The variation in detector location can be seen. In the main plot, the normalized wall current is plotted as a function of bunches in the train: the bunch spacing is fixed at the BIM condition (7 λ_{rf}), and the bunch current is fixed at 2 mA. The vacuum pressure, P, measured near detector 9 is also plotted (located 3 m upstream from EA6). The exponential rise, the number of bunches after which the cloud saturates, and saturation level at 100 mA (total current) all vary; the level varies by up to a factor of three. The inset in the figure shows the cloud build-up at detector 6 when the bunch current is varied.

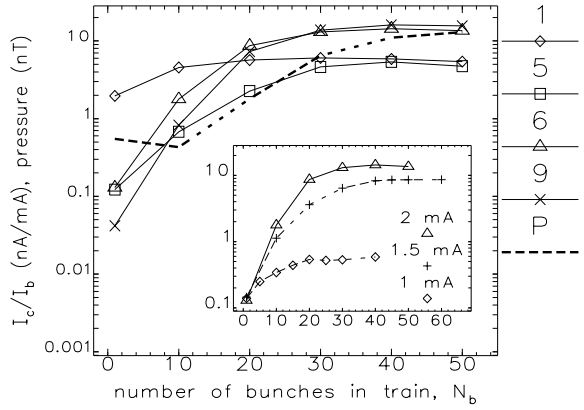

Figure 4: Measured EC build-up and saturation over positron bunch train (main plot: detectors 1, 5, 6, and 9 with 2 mA/bunch; inset: det. 6 only).

From Fig. 4, the cloud density can be very roughly estimated given the measured wall flux and the average electron velocity. It is interesting to compare this to the average beam density. For example, taking 100 mA total current, 2 mA/bunch, and the average energy from the differentiated dI_c/dV, 100 eV (where V is the bias voltage):

$$n_{EC} = I_c / (A_{RFA}\, e \langle v_e \rangle) = 10^4 \text{ cm}^{-3}$$
$$n_{beam} = n_b / A_{vc} / t_{sep} * \text{fill fraction} = 10^6 \text{ cm}^{-3}.$$

Here A_{RFA} is the detector aperture area, ~1 cm^2; A_{vc} is the vacuum chamber cross-section area; t_{sep} is the bunch separation in units of time, $\langle v_e \rangle$ is the velocity of the average-energy electron, 6×10^8 cm/s; and e is the electron charge. Saturation is observed at about 1% of the average beam density for 1.5 and 2 mA/bunch; and at only ~0.1% for 1 mA/bunch.

A preliminary analysis of turn-by-turn beam position monitor (BPM) data acquired during the final run with positrons shows that a horizontal coupled-bunch instability occurs for a bunch spacing 7 λ_{rf} (20 ns) and ~2 mA/bunch; i.e., the BIM conditions. Figure 5 shows the horizontal bunch centroid offset for each of 50 bunches, 90 mA total. Five consecutive turns are shown (ν_x = 0.2). This instability is not observed with electron beams for otherwise identical conditions. Analyses of these data are ongoing.

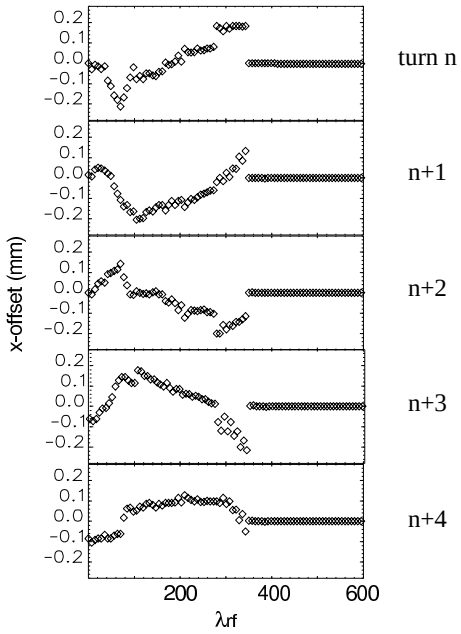

Figure 5: Bunch-by-bunch horizontal centroid oscillations using turn-by-turn BPM data acquisition for positron beam (50 bunches, 90 mA total, BIM spacing). The head of the train is on the left.

4 SIMULATIONS OF EC BUILD-UP

Using the input parameters determined to give the best fit of the measured electron wall current with bunch spacing (Fig. 3), the electron cloud was modeled as a function of bunch train length. The beam model corresponds to the beam conditions in Fig. 4 (fixed bunch current). To study the effects of conditioning of the aluminum chamber surface, two values of δ_{max} were com-

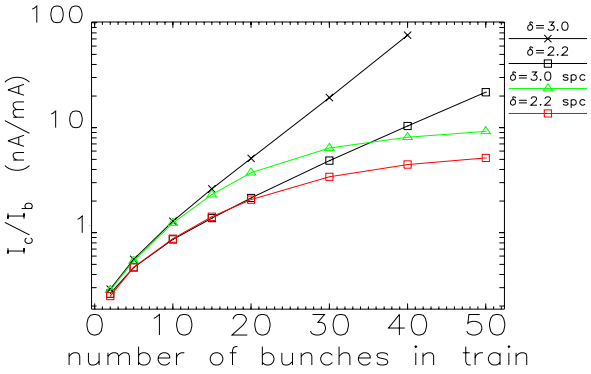

Figure 6: Simulation comparison of δ_{max} and effect of space charge for positron bunch trains in the APS.

pared (recall explanation above Table 1). Finally, the space charge of the cloud was optionally included. The results are shown in Fig. 6. As expected, saturation of the cloud results only when space charge is included, and occurs after about 20 or 30 bunches. The saturation level at 100 mA differs by only a factor of ~2 for the two values of δ_{max}. This would imply that the saturation level is a relatively weak function of this parameter.

The simulated electron cloud build-up can now be compared to the measured data; this is shown in Fig. 7. The fit is reasonably good in the best case (det. 5), shown in (a); however, the fit at the other detectors is marginal, shown in (b). The variation in the electron cloud saturation level as a function of detector location is about as large (3×) as it is for the two chosen values of δ_{max} (2×).

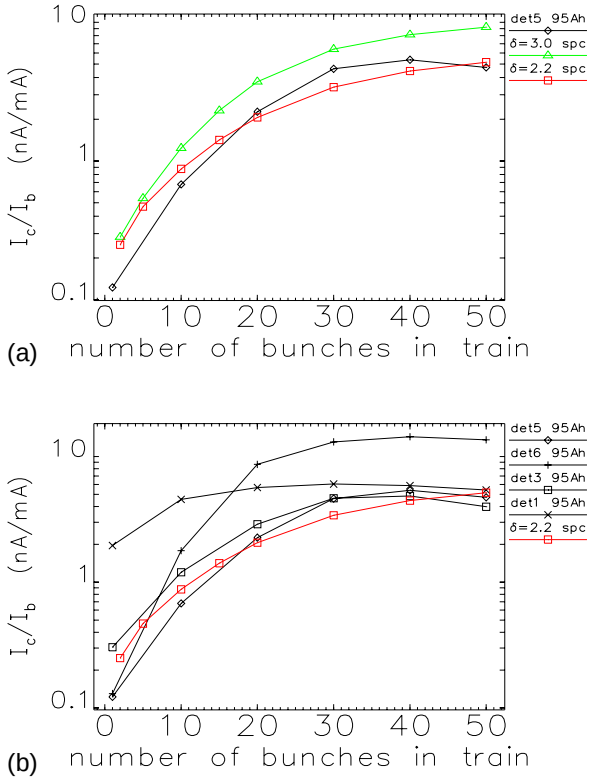

Figure 7: Measured and simulated EC detector current for positron bunch trains: (a) det. 5 and (b) several detectors.

Another test of the model is how well the electron energy spectra are reproduced. A representative set of RFA data showing the integrated electron energy (a) and differentiated signals (dI_c/dV, converted to wall flux) (b) is shown in Fig. 8. The low-energy part of the distributions are fit well with a Lorentzian function. The high-energy part results from electrons accelerated by the beam, and falls off exponentially. For the longest spacing (128 λ_{rf}), there is virtually no exponential tail; we can assume that most of the cloud electrons have been lost before the next bunch passage. For bunch spacings at the BIM resonance, the exponential tail is the longest. Additional features on the tail suggest a resonance condition that "selects" electrons at a certain distance from the beam at each bunch passage, resulting in an energy "peak." A preliminary analysis of the modeled energy spectra shows qualitative similarities to these data. We expect to analyze the measured electron energy distribution in more detail in the future.

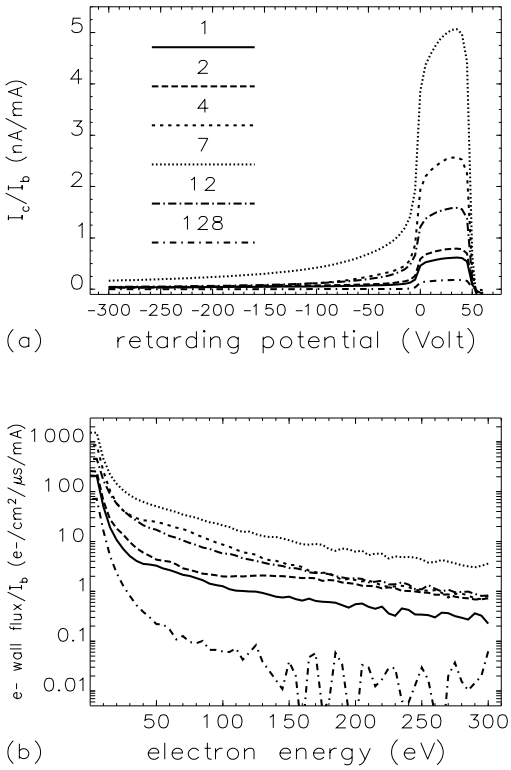

Figure 8: Energy distribution dependence on positron beam operating conditions (ten bunches, constant 2 mA/bunch vs. bunch spacing in units of λ_{rf}); (a) Normalized I_c and (b) dI_c/dV.

5 SUMMARY AND DISCUSSION

A number of observations at the APS have been made for positron and electron beams using dedicated electron diagnostics known as RFAs. These data are being used to help benchmark the code POSINST, developed at LBNL. In summary, electron cloud amplification was observed with positron *and* electron beams (more modest for the latter). A horizontal coupled-bunch instability (CBI) was observed with positron beams at the BIM condition: ~ 2 mA/bunch at a 20-ns bunch spacing (7 λ_{rf}). The instability was not observed for electron beams at these same operating conditions. The EC was observed to saturate after a train of 20–30 bunches at levels varying by up to a factor of three measured at different locations in a field-free region. This variation is primarily due to the influence of a photon absorber. A surface conditioning

effect was observed after a period of beam operation: the electron cloud signal was reduced by a factor of two after an estimated surface electron dose of 2×10^{-4} C/mm^2.

Comparison of simulations with EC measurements have given the following results. Reasonable agreement was found modeling a beam of ten positron bunches whose spacing was varied. The simulation reproduced the shape and position of a broad peak in the collected electron wall current as a function of bunch spacing. It did not, however, reproduce the sharp peak observed at the optimal BIM conditions noted above. The comparison was very sensitive to secondary electron parameters, especially the secondary energy spectrum and the rediffused component.

Using the same secondary electron parameters used to model the BIM resonance described above, the build-up and saturation of the electron cloud over positron bunch trains at the BIM conditions was modeled. To account for surface conditioning effects, different values of δ_{max} were compared, corresponding to conditioned and unconditioned, oxidized Al surfaces. Reasonable qualitative agreement was found compared with the data from one detector. However, the variations observed as a function of detector location were not modeled. This lack of agreement is almost certainly due to geometrical details of the vacuum chamber and photon illumination that are not included in the model. On the other hand, the modeled saturation level varies by a factor of two for a range of values of δ_{max}. The sensitivity of the saturation level to δ_{max} is of the order of the local density variation. The uncertainty in predicting the EC density is thus estimated to be about a factor of two to three.

Given the progress in understanding EC-induced effects at existing accelerators, we may be able to predict EC-induced instability thresholds in future accelerators within an error given by the secondary electron energy spectrum uncertainties, which at present limit a proper parametrization. Including 3D details of the vacuum chamber geometry to model the local EC density variation is also likely to be important. Furthermore, we need to include the important reflected component of the low-energy electrons, which may give an enhancement of the saturation level. This component has not been considered in the simulations shown, but has been included in more recent versions of the POSINST code [9]. Finally, at the APS, a CBI was observed for 2 mA/bunch but not 1.5 mA/bunch, although the estimated average neutralization was the same for both. Other figures-of-merit are clearly important in defining the EC-induced instability threshold.

EC diagnostics have largely been implemented only in field-free regions, with the exception of the CERN Super Proton Synchrotron (SPS) [10]. The EC in the dipoles is considered to be one of the most important contributions to the observed horizontal CBI in that ring; how important is this contribution for positron rings? Electrons trapped in the quadrupole magnet fields may also contribute.

Low-energy (< 5 eV) electrons may never collide with the chamber walls and are thus difficult to measure with a standard RFA. An electron sweeper developed at the PSR was designed to address this issue [11], and experimental results indicate that the properties of this low-energy contribution are very different from those of the multipacting electrons. This question is likely to be a challenge for positron and electron rings as well.

Finally, there is a question as to whether EC instabilities are likely to occur in electron rings. There is an indication that electron cloud build-up does occur for electron beams (e.g., in the APS); the instability threshold may simply be higher in electron rings compared to positron rings.

6 REFERENCES

[1] See other papers presented at this workshop. Additional information can be found in the following workshop proceedings:
Int'l. Workshop on Two-Stream Instabilities in Particle Accelerators and Storage Rings, KEK Tsukuba, Japan, Sept. 2001; http://conference.kek.jp/two-stream/
8th ICFA Mini Workshop on Two-Stream Instabilities in Particle Accelerators and Storage Rings, Santa Fe, NM Feb 2000; http://www.aps.anl.gov/conferences/icfa/two-stream.html

[2] M. A. Furman and G. R. Lambertson, Proc. of Int'l. Workshop on Multibunch Instabilities in Future Electron and Positron Accelerators (MBI-97), KEK, Tsukuba, Japan (Jul. 1997) (KEK Proceedings 97-17, Dec. 1997, 170 and 234); http://www.lbl.gov/~miguel/MBI-97-ECI-PEPII.pdf.
M. A. Furman, Report No. LBNL-41482/CBP Note-247/LHC Project Report 180 (May 1998); http://www.lbl.gov/~miguel/LHCpr180.pdf.

[3] R. A. Rosenberg and K. C. Harkay, Nucl. Instrum. Methods **A453**, 507 (2000).

[4] R. A. Rosenberg and K. C. Harkay, Proc. of 2001 Part. Accel. Conf., 2069 (2001).

[5] K. C. Harkay and R. A. Rosenberg, Proc. of 1999 Part. Accel. Conf., 1641 (1999).

[6] M. Furman, M. Pivi, K. Harkay, R. Rosenberg, Proc. of 2001 Part. Accel. Conf., 679 (2001).

[7] R. Kirby and F. King, Nucl. Instrum. Methods **A469** (1), 1 (2001); also Report No. SLAC-PUB-8212 (Oct. 2000).

[8] V. Baglin, I. Collins, B. Henrist, N. Hilleret, and G. Vorlaufer, Report No. CERN-LHC-Project-Report-472 (Aug. 2001).

[9] M. A. Furman and M. T. F. Pivi, Report No. LBNL-49711/CBP Note-415 (May 2002).

[10] M. Jiminez et al., "Electron Cloud Diagnostics in the SPS Machine," Proc. of Int'l. Workshop on Two-Stream Instabilities in Particle Accelerators and Storage Rings, KEK Tsukuba, Japan, Sept. 2001; http://conference.kek.jp/two-stream/ and "Electron Cloud Observations in the SPS," these proceedings.

[11] R. Macek et al., Proc. of 2001 Part. Accel. Conf., 688 (2001).